Analytical assessment of the load carrying capacity of axially loaded wooden reinforced tubes

J. M. Cabrero [a,*,1] A. Heiduschke [b] P. Haller [b]

[a] *Department of Structural Analysis and Design, School of Architecture, University of Navarra, 31080 Pamplona, Spain*

[b] *Timber Construction Institute, Technische Universität Dresden, 01062 Dresden, Germany*

Abstract

As a natural resource, an efficient use of wood should be also a requirement for structural timber design, but the usual structural solid sections do not achieve the required optimal behaviour. The performance of the structural elements (serviceability and strength) depends not only on the material properties, but mainly on the moment of inertia of the cross section. The Timber Construction Institute of Technische Universität Dresden has developed a process for the manufacture of structural wood profiles. The resulting profiles combine economy, an efficient use of the material and optimal structural performance. They are externally reinforced with composite fibres, which improve the mechanical characteristics of the wood and protect it from weathering. The available experimental tests to axial loading show the outstanding properties of this new technology. Herein, the preliminary model developed to obtain the axial strength of longitudinally compressed tubes is presented. Two different analytical algorithms are discussed and applied. The model adequately predicts the

axial strength of fibre reinforced wood profiles. The analytical results are within an error less than 10% to the available experimental results, with a mean error ratio less than 3%.

Key words: Efficiency, Wood, Glass fibre, Analytical models, Axial strength, Tsai-Wu failure criteria

---

Nomenclature

Greek letters

η	Stress partitioning parameter
γ_{unr}	Reduction factor for the unreinforced tubes
λ	Slenderness ratio
ν	Poison's ratio
$\left[\epsilon\right], \left\{\epsilon\right\}$	Strain vector
$\left[\kappa\right], \left\{\kappa\right\}$	Curvature vector
$\left[\sigma\right], \left\{\sigma\right\}$	Stress vector

* Corresponding author. Tel.: +34-948425600-2725; fax: +34-948425629
Email addresses: jcabrero@unav.es (J. M. Cabrero),
andreas.heiduschke@tu-dresden.de (A. Heiduschke),
peer.haller@tu-dresden.de (P. Haller).

[1] Supported by the Alexander von Humboldt Foundation

Upper cases

$\left[A\right]$	Tensile in-plane stiffness matrix
$\left[B\right]$	Coupling in-plane stiffness matrix
CLT	Classical Laminate Theory
$\left[D\right]$	Flexural in-plane stiffness matrix
D	Ductility index
E	Young's modulus (MOE)
F_{ij}, F_i	Strength parameters in stress space
FPF	First Ply Failure
G	Shear modulus
G_{ij}, G_i	Strengths parameters in strain space
R	Strength/stress ratio for Tsai-Wu failure criteria
$\left[S\right]$	In-plane stiffness matrix
S	Longitudinal shear strength
V	Volume ratio
V_i^*	Stress partitioning parameter for the i direction
X	Longitudinal tension strength
X'	Longitudinal compression strength
Y	Transversal tension strength
Y'	Transversal compression strength

Lower cases

h	Total thickness of laminate

m	Number of plies
r	Outer radius of the tube
r_m	Mean radius of the axis of the tube
t	Wall thickness
z	Axis transverse to the plane of a laminate, thickness coordinate of the ply

Indexes

$*$	Normalized matrix
1	xx normal stress/strain, in contracted notation
2	yy normal stress/strain, in contracted notation
6	xy shear stress/strain, in contracted notation
$comp$	Compression
CR	Related to the composite reinforcement
f	Related to the fibre of the composite
$fail$	Failure
ini	Initial unloaded state
L, 0	Longitudinal direction of the wood
m	Bending
m	Related to the matrix of the composite
$norm$	Normalized
R, 90	Radial direction of the wood
REF	Unreinforced tube, used as reference
s	Shear

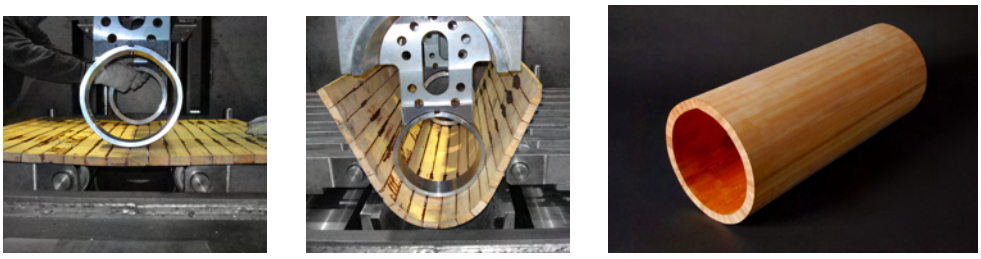

(a) (b) (c)

Fig. 1. Wood tubes: (a) and (b), manufacturing process; (c) unreinforced wood tube.

T, 90	Tangential direction of the wood
tens	Tension
unr	Unreinforced
W	Related to the wood
x	Direction x of the material (usually, longitudinal, direction of the grain)
y	Direction y of the material (usually, transversal, perpendicular to the grain)

1 Introduction

Our design objectives are increasingly determined by the need of a sustainable economical development. Thus, an efficient use of the available materials becomes increasingly important. Apart from the material properties, the structural and economical performance of the cross section is the most important design issue.

Structural elements must safely transfer forces and moments and simulta-

neously meet the serviceability requirements. The moment of inertia of the section is a major parameter for both required tasks. However, in the case of timber, by means of the traditional transformation technologies (sawing...), round or square solid cross sections are produced. These traditional cross sections are less competitive and efficient when compared to more engineered sections, such as steel profiles.

From those thoughts, a procedure of manufacturing formed wooden profiles has been developed and patented [1]. Wood is compressed in its transverse direction up to 50% of its original size by folding its microstructure. This densification process is reversible, and it becomes the principle of this innovative manufacturing process, where glued laminated thick solid panels of densified wood are transformed to open or closed prismatic cross sections by reversing the compression applied by means of heat and moisture and moulding [1] (Fig. 1). This manufacturing principle may be applied to a wide variety of sections: all open and closed prismatic cross-sections may be produced in a continuous manufacturing process with the appropriate pattern. The resulting profile encompasses efficient use of the material and optimal structural performance. The here proposed and analysed circular hollow sections (Fig. 1c) behave well when subjected to axial forces, so they are well suited for columns.

Depending on the wall thickness of the timber profile, an additional fibre reinforced plastic (FRP) glued to the outer surface of the profile might be required to strengthen the wood [1]. Thin walled profiles are prone as well to develop longitudinal cracks due to shear and tensile stresses perpendicular to the grain. Load adapted FRP reinforcement can avoid brittle type failures of the profiles. Consequently, wood profits from the outstanding mechanical and physical characteristics of FRP. Wood profiles are well suited for the use in

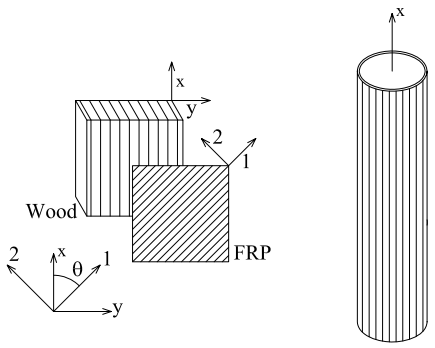

Fig. 2. Used coordinate systems: $x-y$ axes refer to material coordinates of the wood (whose grain direction, x, corresponds to the longitudinal of the tube), $1-2$ axes refer to local coordinates of each FRP ply.

light-weight structures — the classical field of FRP composites. Their use as a permanent winding core can help to reduce manufacturing costs. The wooden core will eliminate local buckling effects and strengthen the FRP profile in axial direction.

The presented research work deals with the development of an analytical model to obtain the axial strength for the design of the wooden tubes reinforced with glass-fibre–epoxy composite subjected to simple axial compression loading. The model results are compared to the available experimental results [2,3].

2 Theoretical background

2.1 Classical Laminate Theory

The Classical Laminate Theory (CLT) (described, among others, in [4–7]) is employed herein to determine the properties of the composite material, made from the wood and the FRP reinforcement.

The theory is based on the laminate plate theory for thin, flat laminates undergoing small deformations. The following assumptions apply: strains vary linearly across the laminate; out-of-plane shear deformations are negligible; and the out-of-plane normal stress σ_z and the shear stresses τ_{xz}, τ_{yz} are small when compared with the in-plane σ_x, σ_y and τ_{xy} stresses. By these assumptions, plane stress conditions are applied. Kirchoff hypothesis is assumed as well, and consequently normals to the reference surface are considered to remain normal and straight.

The absolute stiffness matrix for a laminate, $\left[S\right]$, is defined as

$$\begin{Bmatrix} \left[N_i\right] \\ \left[M_i\right] \end{Bmatrix} = \begin{bmatrix} \left[A_{ij}\right] & \left[B_{ij}\right] \\ \left[B_{ij}\right] & \left[D_{ij}\right] \end{bmatrix} \begin{Bmatrix} \left[\epsilon_j^0\right] \\ \left[\kappa_j\right] \end{Bmatrix} = \left[S\right] \begin{Bmatrix} \left[\epsilon_j^0\right] \\ \left[\kappa_j\right] \end{Bmatrix}, \tag{1}$$

where $\left[A\right]$, $\left[B\right]$ and $\left[D\right]$ are the in-plane tensile, coupling and flexural stiffness matrices of the resulting laminate. They are obtained from summation of the m plies and the elements of the bidimensional plane-stress stiffness matrix of each ply, $\left[Q\right]$, as follows

$$\left[A\right] = \sum_{i=1}^{m} \left[Q_i\right] (z_i - z_{i-1}) \tag{2a}$$

$$\left[B\right] = \frac{1}{2} \sum_{i=1}^{m} \left[Q_i\right] \left(z_i^2 - z_{i-1}^2\right) \tag{2b}$$

$$\left[D\right] = \frac{1}{3} \sum_{i=1}^{m} \left[Q_i\right] \left(z_i^3 - z_{i-1}^3\right), \tag{2c}$$

where $\left[Q\right]$ is the plane stress stiffness matrix of the ply material,

$$\left[Q\right] = \begin{bmatrix} \frac{E_x}{1-\nu_x\nu_y} & \frac{\nu_y E_x}{1-\nu_x\nu_y} & 0 \\ \frac{\nu_x E_x}{1-\nu_x\nu_y} & \frac{E_y}{1-\nu_x\nu_y} & 0 \\ 0 & 0 & G \end{bmatrix} \tag{3}$$

2.1.1 Normalized matrix for a laminate

Tsai [4] proposed, instead of the previously defined (and usually employed) absolute matrix (1), the use of a normalized stiffness matrix:

$$\left[S_{norm}\right] = \begin{bmatrix} \left[A^*_{ij}\right] & \left[B^*_{ij}\right] \\ 3\left[B^*_{ij}\right] & \left[D^*_{ij}\right] \end{bmatrix}, \tag{4}$$

where the normalized matrices are defined as

$$\left[A^*\right] = \frac{1}{h}\left[A\right] \tag{5a}$$

$$\left[B^*\right] = \frac{2}{h^2}\left[B\right] \tag{5b}$$

$$\left[D^*\right] = \frac{12}{h^3}\left[D\right]. \tag{5c}$$

The normalization of the in-plane, $\left[A\right]$, and the flexural, $\left[D\right]$, matrices follows the usual convention: the in-plane matrix is normalized by the laminate thickness, h, and the flexural by the moment of inertia of a rectangular section. The applied normalization factor in the case of the coupling matrix, $\left[B\right]$, corresponds to that of a normalized moment of inertia for a rectangular

section.

The resulting normalized matrix $\left[S_{norm}\right]$ (4), is not symmetric, but, as an advantage, its units are uniform. All normalized stress and stiffness have the same units, i.e. in Pa, while the strains are dimensionless. Consequently, this matrix allows for direct comparison of the stiffness components. In the absolute representation of the matrix, $\left[S\right]$ (1), the different partial matrices have different units; e.g. $\left[A\right]$ in N/mm, $\left[B\right]$ in N, and $\left[D\right]$ in Nmm.

The previously defined matrices, $\left[A\right]$, $\left[B\right]$ and $\left[D\right]$ (2), represent the stiffness of a laminate, and describe its response to moments and in-plane forces. They also depict the different types of couplings which may arise in a laminate[6]. Some of them are characteristic of composite materials, and they do not occur in homogeneous isotropic materials, like the extension-shear (A_{16}, A_{26} –the reader should be aware that contracted numeral notation [4], where subscript 1 refers to xx, 2 to yy, and 6 to xy, is used in this paper–), the bending-twist (D_{16}, D_{26}), the extension-twist and bending-shear (B_{16}, B_{26}), and the in-plane–out-of-plane couplings (B_{ij}). Since twist deformations cannot exist in a closed cylindrical surface [8], the corresponding coupling parameters, B_{16} and B_{26} in $\left[B\right]$, are not relevant for the wood profiles in this study.

The two remaining couplings occur in both composite and isotropic materials, and they are the extension-extension (A_{12}, which corresponds to Poison's effect), and the bending-bending coupling (D_{12}).

2.2 Tsai-Wu Failure criteria

The Tsai-Wu failure criteria [4,11] is extensively employed for the design of composite structures. It is a quadratic failure criteria, based on the tensor theory, whose general formula for an orthotropic or transversely isotropic ply under plane stress is

$$F_{ij}\sigma_i\sigma_j + F_i\sigma_i = 1. \tag{6}$$

This general equation, when expanded for an orthotropic material (in which $F_{xs} = F_{ys} = F_s = 0$) submitted to plane stress, leads to:

$$F_{xx}\sigma_x^2 + 2F_{xy}\sigma_x\sigma_y + F_{yy}\sigma_y^2 + F_{ss}\sigma_s^2 + F_x\sigma_x + F_y\sigma_y = 1. \tag{6'}$$

In (6'), and in this paper as well, contracted notation as defined by Tsai [4] is employed (i.e. $\sigma_{xx} \equiv \sigma_x$, $\sigma_{xy} \equiv \sigma_s$).

The different parameters, F_{ij}, required in (6') are defined based on the different strength properties of the material.

$$F_{xx} = \frac{1}{XX'} \tag{7a}$$

$$F_x = \frac{1}{X} - \frac{1}{X'} \tag{7b}$$

$$F_{yy} = \frac{1}{YY'} \tag{7c}$$

$$F_y = \frac{1}{Y} - \frac{1}{Y'} \tag{7d}$$

$$F_{ss} = \frac{1}{S^2}. \tag{7e}$$

The term F_{xy}, known as the interaction term, is defined as

$$F_{xy} = F_{xy}^*\sqrt{F_{xx}F_{yy}} \tag{8}$$

To achieve a closed failure envelope, the condition

$$-1 \leq F_{xy}^{*} \leq 1 \tag{9}$$

must be fulfilled. This is required to assure that the failure criterion is valid for any possible stress state.

2.2.1 Strain space

In the present work, the Tsai-Wu criterion in strain space is used. When expressed in the strain space, it is an invariant for a given ply angle. It may be thus viewed as a material property, and it may be easily used to analyse ply failure, since the CLT (Sect. 2.1) is applied just by superimposing the failure criteria for each ply. Its general formula is analogous to the previously given for the stress space, (6):

$$G_{ij}\epsilon_i\epsilon_j + G_i\epsilon_i = 1, \tag{10}$$

when expanded:

$$G_{xx}\epsilon_x^2 + 2G_{xy}\epsilon_x\epsilon_y + G_{yy}\epsilon_y^2 + G_{ss}\epsilon_s^2 + G_x\epsilon_x + G_y\epsilon_y = 1 \tag{10'}$$

The parameters G_{ij} are based on the previously defined strength parameters

F_{ij} given in (7),

$$G_{xx} = F_{xx}Q_{xx}^2 + 2F_{xy}Q_{xx}Q_{xy} + F_{yy}Q_{xy}^2 \tag{11a}$$

$$G_{yy} = F_{xx}Q_{xy}^2 + 2F_{xy}Q_{xy}Q_{yy} + F_{yy}Q_{yy}^2 \tag{11b}$$

$$G_{xy} = F_{xx}Q_{xx}Q_{xy} + F_{xy}Q_{xx}Q_{yy} + Q_{xy}^2 + F_{yy}Q_{xy}Q_{yy} \tag{11c}$$

$$G_{ss} = F_{ss}Q_{ss}^2 \tag{11d}$$

$$G_x = F_xQ_{xx} + F_yQ_{xy} \tag{11e}$$

$$G_y = F_xQ_{xy} + F_yQ_{yy}. \tag{11f}$$

The Q_i parameters correspond to plane stress stiffness matrix, as previously defined in (3).

The failure envelope for each ply (expressed in $1-2$, *ply axes*, see Fig. 2) may be transformed into the selected coordinate system [4] ($x-y$, also referred as the *laminate*, and where axis x corresponds both to the longitudinal direction of the tube and that of the grain of the wood, see Fig. 2).

$$\begin{Bmatrix} G_{11} \\ G_{22} \\ G_{12} \\ G_{66} \\ G_{16} \\ G_{26} \end{Bmatrix} = \begin{bmatrix} m^4 & n^4 & 2m^2n^2 & 4m^2n^2 \\ n^4 & m^4 & 2m^2n^2 & 4m^2n^2 \\ m^2n^2 & m^2n^2 & m^4+n^4 & -4m^2n^2 \\ m^2n^2 & m^2n^2 & -2m^2n^2 & (m^2-n^2)^2 \\ m^3n & -mn^3 & mn^3-m^3n & 2\,(mn^3-m^3n) \\ mn^3 & -m^3n & m^3n-mn^3 & 2\,(m^3n-mn^3) \end{bmatrix} \begin{Bmatrix} G_{xx} \\ G_{yy} \\ G_{xy} \\ G_{ss} \end{Bmatrix}, \tag{12}$$

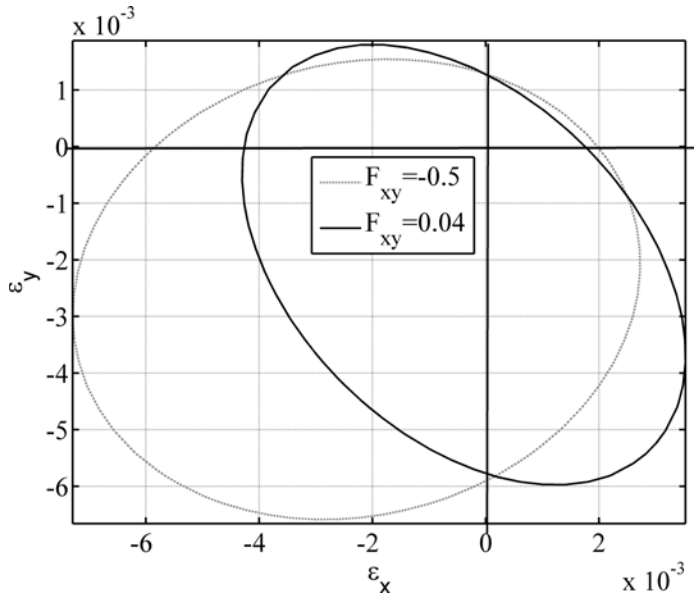

Fig. 3. Influence of the interaction factor in the failure envelope of the wood (strain space).

and

$$\begin{Bmatrix} G_1 \\ G_2 \\ G_6 \end{Bmatrix} = \begin{bmatrix} m^2 & n^2 \\ n^2 & m^2 \\ mn & -mn \end{bmatrix} \begin{Bmatrix} G_x \\ G_y \end{Bmatrix} \tag{13}$$

where

$$m = \cos\theta \tag{14a}$$

$$n = \sin\theta \tag{14b}$$

$$\theta = \text{rotation angle between coordinate systems, see Fig. 2} \tag{14c}$$

2.2.2 Interaction term for the wood

In the present research, the wood was treated as a composite material. Consequently, an adequate interaction factor F^*_{xy} for wood had to be applied. Tsai [4] recommends, in absence of good data, the following value $F^*_{xy} = -0.5$, which

corresponds to a generalised von Mises criterion. The question is whether this value proves adequate or not for wood. In [9], a zero interaction factor is proposed for wood.

Eberhardsteiner [10] accomplished an extensive experimental program on the failure behaviour of clear spruce. A 2nd-order curve, of the same form as that in (6'), was fitted on the experimental failure results. Based on these experimental results, the interaction factor for clear spruce wood, F_{xy}^{*} (8), may be thus inferred as

$$F_{xy}^{*} \approx 0.04. \tag{15}$$

This value may be regarded (due to the extensive research accomplished in [10]) as a representative interaction term for spruce wood. It differs to a great extent from the value proposed by [4]. It is close to a zero value, as proposed in [9]. The different resulting envelopes for both interaction factors are depicted in Figure 3. They clearly differ in the 3rd quadrant (where $\sigma_y < 0$ and $\sigma_x < 0$, compression perpendicular and longitudinal to the grain), where the new proposal ($F_{xy}^{*} \approx 0.04$) is quite more restrictive.

In the 2nd (where $\sigma_y > 0$, tension perpendicular to the grain) and 4th quadrants, due to the resulting rotation, the proposed interaction term allows for higher strains before failure.

As explained, the failure envelopes in the strain space are invariant [4]: with independence of the presence of other plies, their shapes remain the same. The failure of a laminate is then simply produced by superimposing the failure of its plies, adequately transformed taking into account their corresponding orientation (as shown in (12) and (13)).

The inner envelope of all the ply-failures corresponds to the First Ply Failure (FPF). It describes the maximum capability of the intact plies. It is usually employed in the design of composite materials as the design capacity of the material.

But FPF does not necessarily mean the ultimate load. The remaining plies, which have not yet failed, may continue carrying load beyond. The determination of the Last Ply Failure (LPF) would require the analysis of progressively degraded plies, and it is not accomplished in the present paper.

2.2.3 Strength ratio

The strength/stress ratio R [4,11] is the ratio between the maximum allowable stress and the applied stresses. It gives a direct measure of the security factor for the applied loads. Hence, it must be assumed that the material response is linearly elastic. Proportional loading is as well required, so that all components of stress and strain increase by the same proportion. This latter condition means that the loading vectors in stress and strain space are kept in the same direction.

The Strength Ratio, R, may be obtained by substituting the maximum stress components into the failure criterion [11], by means of the following relation

$$R\sigma_i|^{applied} = \sigma_i|^{max}, \tag{16}$$

the failure criterion takes the form when the maximum failure values are reached

$$F_{ij}\sigma_i|^{max}\sigma_j|^{max} + F_i\sigma_i|^{max} = 1 = \left[F_{ij}\sigma_i|^{applied}\sigma_j|^{applied}\right]R^2 + \left[F_i\sigma_i|^{applied}\right]R \tag{17}$$

By solving the expression (17) for R, the Strength Ratio is obtained:

$$R = -\frac{b}{2a} + \sqrt{\left(\frac{b}{2a}\right)^2 + \frac{1}{a}} \tag{18}$$

where

$$a = F_{ij}\sigma_i|^{applied}\sigma_j|^{applied} \tag{19a}$$

$$b = F_i\sigma_i|^{applied} \tag{19b}$$

As defined in [4], only positive values may occur. Based on the definition of the Strength Ratio, (17), when $R = 1$ failure occurs. For higher values, $R > 1$, the material has not yet failed, and its value provides a measure of the safety factor of the structure (as long as the previously explained assumptions remain valid).

3 Experimental results

3.1 Mechanical properties of the materials

3.1.1 Wood

Partially densified spruce wood was used for the tubes. Clear small specimens for the wood were obtained and tested to simple compression and bending, according to DIN standards [12,13]. The mean value for the compression strength was 60.5N/mm^2, with a standard deviation of 12.1N/mm^2. The 5-percentile compression strength was 43.5N/mm^2.

The mean elastic modulus was determined in 16 150N/mm^2 (the standard

Table 1

Mean ratios between the strength properties of the wood, based on the ratios from [15–17].

X_{tens}	Y_{tens}	X_{comp}	Y_{comp}	S_{xy}	Bending
0.6951	0.0289	1.0000	0.1295	0.1283	0.8922

deviation was 930N/mm^2). Based on the experimental Young's modulus, the remaining elastic properties were obtained. The usual relations, as proposed in [14], were employed:

$$E_L : E_R : E_T \approx 20 : 1.6 : 1 \tag{20a}$$

$$G_{LR} : G_{LT} : G_{RT} \approx 10 : 9.4 : 1 \tag{20b}$$

$$E_L : G_{LR} \approx 14 : 1 \tag{20c}$$

Only the compressive and bending strengths were obtained in the tests. The remaining strength properties were derived from the compression strength, based on relations derived from [15–17] (given in Table 1), are shown in Table 2.

The tension strength perpendicular to the grain is one of the critical factors for the modelling of wood. The results of a comprehensive study for solid and laminated wood cross-sections are given in [18]. The derived value for this property (Table 2), 1.4N/mm^2, is lower than the mean value given in [18] for solid wood (1.89N/mm^2), and it is slightly lower than the maximum for laminated wood given in [18] (1.42N/mm^2). Since partially densified wood is used, the derived value for this property seems adequate.

3.1.2 Composite reinforcement

The material properties for the composite material employed as reinforcement in the wooden tubes are obtained by means of the two component materials: the E-Glass fibre and the epoxy resin matrix.

The elastic properties for the E-Glass fibre are obtained from [19]. They correspond to the standard values given for this material. The values for the epoxy resin (LN-1, produced by Vosschemie) are those given by the manufacturer, and locate between the usual properties. A fibre volume of 0.33 is employed.

The micromechanics formulae in [4] are employed to derive the elastic properties of the composite:

$$E_x = V_f E_{f,x} + V_m E_m \tag{21}$$

$$\nu_x = V_f \nu_f + V_m \nu_m \tag{22}$$

$$E_y = \frac{1 + V_y^*}{\frac{1}{E_{f,y}} + \frac{V_y^*}{E_m}} \tag{23}$$

$$G_s = \frac{1 + V_s^*}{\frac{1}{G_{f,x}} + \frac{V_s^*}{G_m}} \tag{24}$$

Derivation of the longitudinal properties, E_x (21) and ν_x (22), are based on the usual rule of mixtures. They correspond to a parallel model, where the longitudinal fibre and matrix strains are assumed to be equal.

The transversal properties, E_y and G_s, (23) and (24), are based on a modified rule of mixtures, as proposed in [4]. They are based on a series model, where the same stress is assumed for all the components. A stress partitioning parameter, η, thought as the ratio of the average matrix to average fibre stresses,

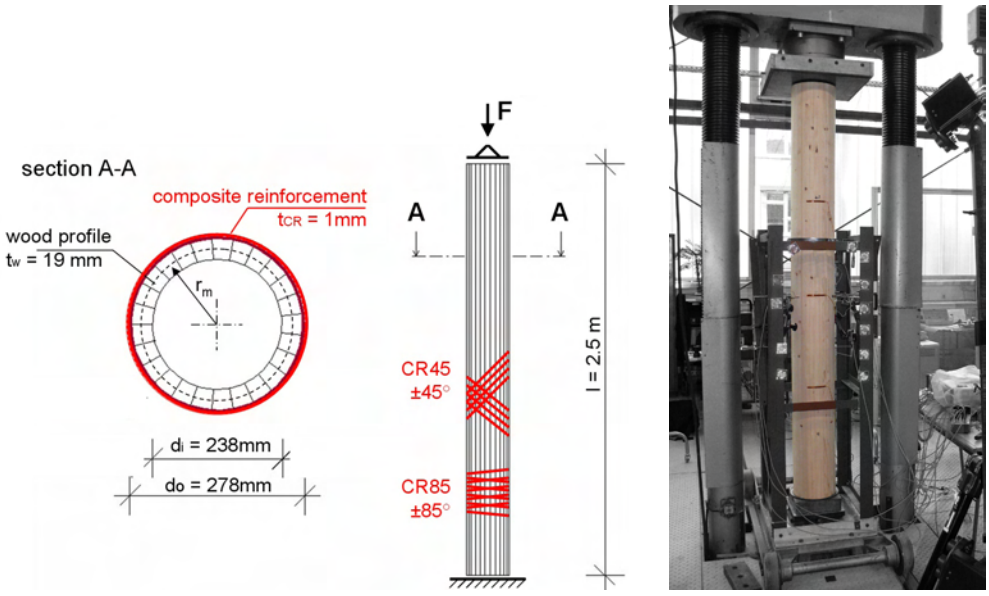

(a) (b)

Fig. 4. Dimensions of the tube (a) , and test set-up (b).

is added [4].

$$V_y^* = \eta_y \frac{V_m}{V_f} \tag{25}$$

$$V_s^* = \eta_s \frac{V_m}{V_f} \tag{26}$$

It is an empirical constant, which may be back-calculated from the experimental data by assuming the fibre (alone) as isotropic. Tsai [4] derived the values $\eta_y = 0.516$ and $\eta_s = 0.316$ for a glass-epoxy composite. These are the values used in this research. The derived material properties are given in Table 2

3.2 Previous experimental results

Previously to the model development, herein described five tubes, one unreinforced reference specimen (REF) and four composite reinforced tubes (CR) were tested in axial compression [2]. The columns with a total length of 2.5m

Table 2

Material properties employed

Material Properties	Abbr.	Unit	Wood (partially densified)	Composite Reinforcement
Density	ρ	[kg/m^3]	582(110)*	1800
Bending Strength	$\sigma_{m,0}$	[N/mm^2]	105.2(18.6)*	240[a]
Compression strength	$\sigma_{c,0}$	[N/mm^2]	60.5(12.1)*	240[a]
	$\sigma_{c,90}$		7.5	70[a]
Tensile Strength	$\sigma_{t,0}$	[N/mm^2]	55.9	240[a]
	$\sigma_{t,90}$		1.4	50[a]
Shear Strength	σ_{xy}	[N/mm^2]	8.8	25[a]
Modulus of Elasticity	E_0	[N/mm^2]	16150(930)∗	26600
	E_{90}		1340	6900
Shear Modulus	G_xy	[N/mm^2]	840	3000
Poison Ratio	ν_{xy}	–	0.04	0.07
	ν_{yx}		0.35	0.26

* mean value from 9 experiments (standard deviation)

[a] irrelevant parameter

$x \equiv$ direction of the grain (wood) $\equiv$ longitudinal (0°)

$y \equiv$ direction perpendicular to the grain (wood) $\equiv$ tangential $\equiv$ radial (90°)

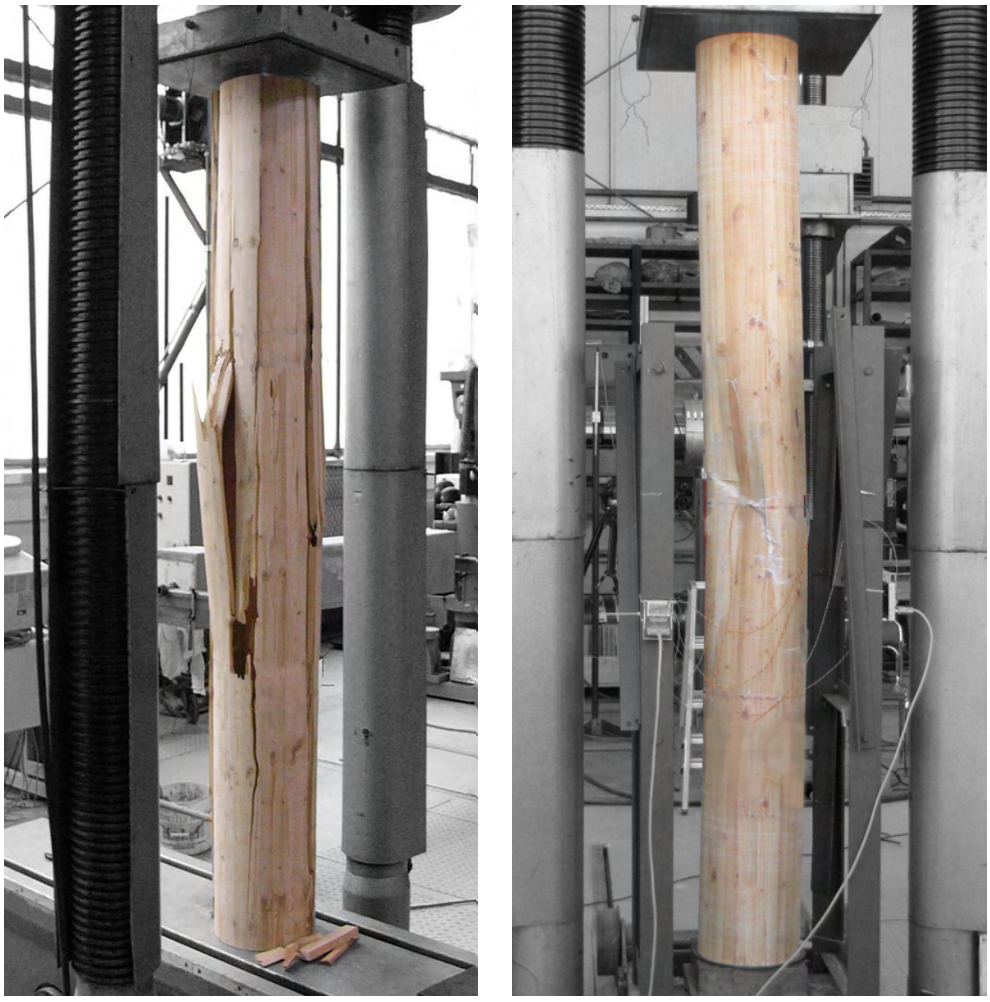

(a) (b)

Fig. 5. Failure modes: (a) splitting of REF tube, (b) local buckling of CR85 tube

and a slenderness ratio of 27 were tested in a 6MN hydraulic press. The dimensions of the specimen including the orientation of the fibre reinforcement and the test set-up of a 2.5m column are shown in Figure 4.

The supporting plate at the bottom of the column was fixed while the upper plate was pin-supported. The steel frame surrounding the specimen was not connected to the tube. It was used to attach measurement devices (displacement transducers) and to protect the equipment from possible damagen (Fig. 4b).

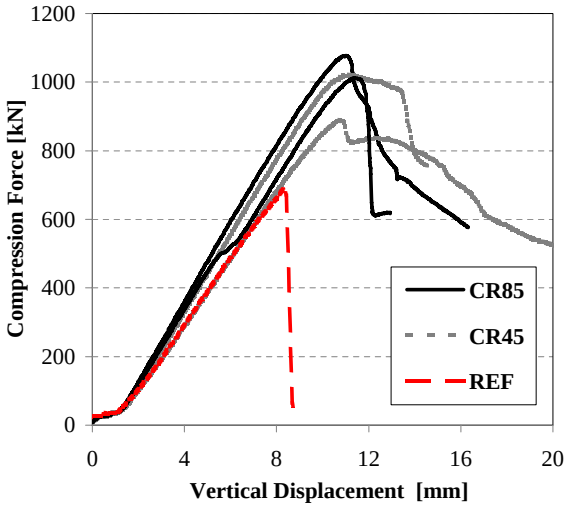

Fig. 6. Experimental load-deformation curves

With a radius r_m of 129mm and a wall thickness t_w of 19mm (Fig. 4a) the tubes can be classified as moderate thick cylinders [20]. The self-weight of the tubes was in average 30kg, inclusive 4kg composite confinement. The reinforcement was laminated to the outer wood surface in a filament winding process. The thickness t_{CR} of the transparent glass fibre-epoxy composite layer was about 1mm. The glass-fibre yarns were oriented in an angle of $\pm 45°$ (CR45) and/or $\pm 85°$ (CR85) to the column axis. The weight per area of the glass fibres was $900 \mathrm{g/m^2}$.

Fig. 6 shows the load-deformation curves of the columns. The reference tube exhibited brittle failure at a load level of 685kN. This corresponds to a compression failure stress of $44.7 \mathrm{N/mm^2}$.

The experimental results of the reinforced columns reveal that the load-carrying capacity and ductility can be significantly enhanced by means of the composite confinement. In average the reinforced tubes reached a maximum load of 1 000kN. In comparison to the reference, the load-carrying capacity of the reinforced columns increased by factors of 1.46 and 1.22 for the CR85 and CR45

tubes, respectively. In regard to the stiffness of the column the presence of reinforcement is negligible.

The reference tubes exhibited brittle failure by splitting of the wood section into a number of single lamellas - see Figure 5a. This separation is a result of tensile stresses in perpendicular to grain (hub) direction due to the Poisson-effect and the corresponding increase in diameter of the axially loaded tubes. The load-deformation behaviour until failure is linear elastic resulting in a ductility D of 1, where D is defined as the relation between yield displacement and ultimate displacement.

In contrast to the reference, no brittle failure was observed for the composite reinforced columns. It was found that the cross sections ovalize before failing in compression due to the crushing of wood fibres parallel to grain resulting into a final local buckling failure mode (Figure 5b). Plastic capabilities were observed for all of the reinforced tubes, where especially the CR45 tubes can be classified as ductile. The ductility D was 1.4 and 1.1 for CR45 and CR85, respectively.

The specimen described above will be referred in this document as series A. In another previous experimental campaign [21] thirteen unreinforced reference and sixteen reinforced tubes were subjected to axial compressions. In contrast to CR45 and CR85, common woven glass-fibre fabrics with a fibre orientation of $0°/90°$ was used for to reinforce the CR090 tubes. These tubes are called series B in this document. A detailed description of the specimen and experimental results can be found in [3].

4 Algorithm of the model

The experimental results (Fig. 6) show how the tube with a $\pm 85°$ reinforcement fails, when submitted to a simple compressive load, at a higher load than that with a $\pm 45°$ reinforcement.

When a standard cylindrical tube is submitted to a simple longitudinal compressive load, two different deformations arise. The most important is in the longitudinal direction, and it is due to the compressive load. A second deformation is produced: an expansion in the transversal (radial) direction of the tube. This latter deformation is usually disregarded. However, it may not be dismissible in the case of thin-walled wood profiles. It is mainly due to the Poison effect: the material deforms in a direction perpendicular to that of the load application.

The failure of the unreinforced tubes (Figure 5a) corresponds to this transversal deformation, which results in tension perpendicular to the grain. The high orthotropy of the wood must also be taken into account: its transversal elastic modulus is about 20 times lower than the longitudinal one (20a). The transversal strength is much lower as well, 20 (in tension) and 7 (in compression) times lower (Table 1).

4.1 Assumptions

An analytical procedure to obtain the axial failure load of the tubes, based on the theories briefly explained in previous Sect. 2.1 and 2.2 is developed. The response of the tubes, and the experimentally observed transversal displace-

ments are assumed to be only because of the Poison effect in the material. The proposed model applies the general laminate plate theory to obtain the material properties and the Tsai-Wu failure criteria to predict the failure. The employed algorithm is shown in Fig. 7.

The radius-thickness ratio is $r/t \approx 7.7$. The analysed tubes may be considered as moderately thick shells, for which it would be usually assumed that CLT is not applicable [20]. However, taking into account the particular characteristics of the studied laminate (made from only two layers, one moderately thick of wood, and an outer thin of FRP), and since a preliminary analytical model is aimed, Love's first approximation is assumed (the difference in the areas of shell wall elements above and below the middle surface is neglected [22]).

The material is assumed to be linearly elastic; for each state of combined stresses there is a corresponding state of combined strains; proportional loading is assumed –all the components of stress and strain increase by the same proportion (similarly to the assumption made in the Strength Ratio definition, see Sect. 2.2.3)–.

4.2 Graphical procedure

Figure 8 depicts the algorithm in a graphical way. In the strain space, the Tsai-Wu failure criteria of the layers of a composite material is plotted. Strain space must be used, since both layers (in a thin shell theory) share the strain when submitted to axial loading. And also, the failure envelope of the layer is an invariant in the strain space. Given a state of strain, $\left\{ \epsilon_A \right\}$, it may be easily plotted into the graph as point **A** when both coordinates, $(\epsilon_{x.A}, \epsilon_{y.A})$,

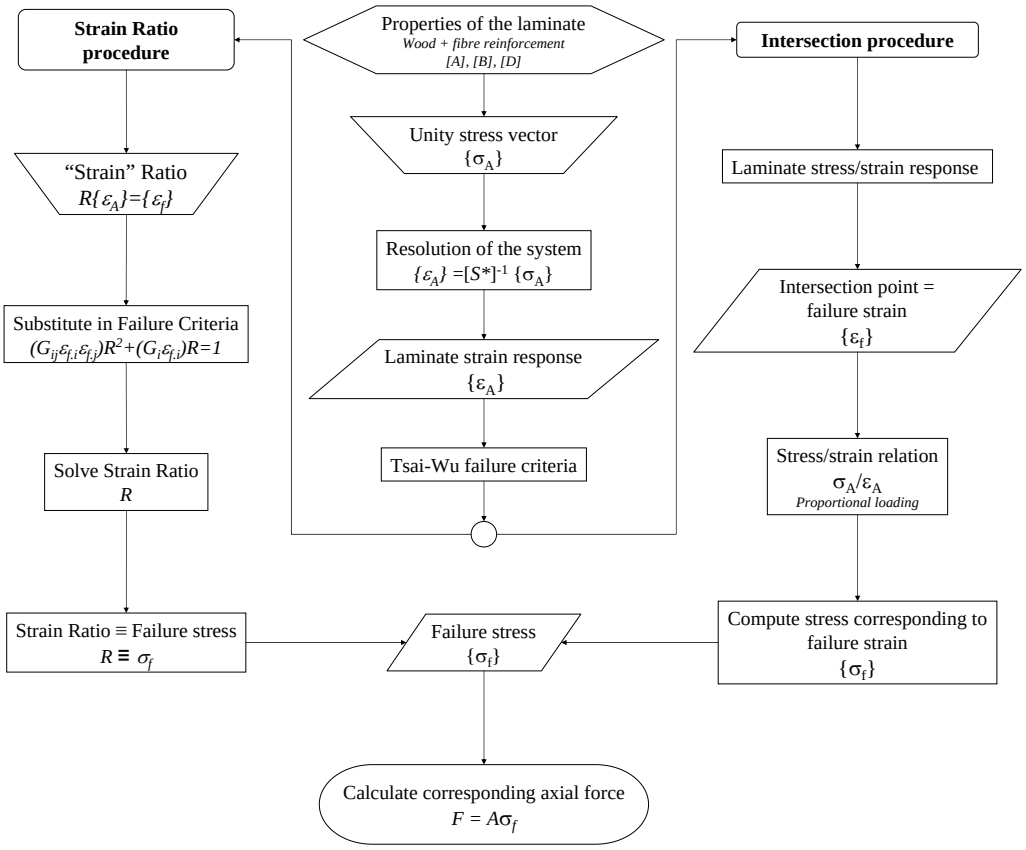

Fig. 7. Algorithm applied to obtain the strength of the tubes

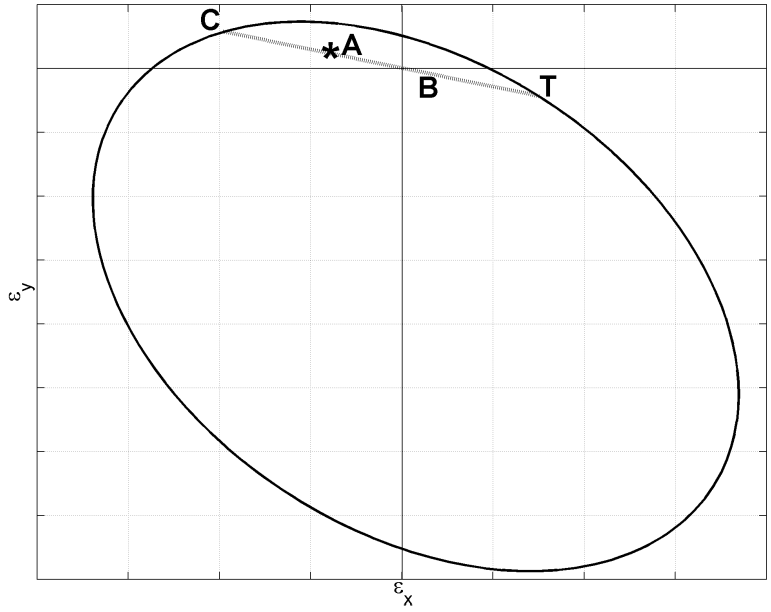

Fig. 8. Graphical application of the analytical model

are known. It is assumed that for this strain state, the corresponding stress state is known, and given in a stress vector $\left\{ \sigma_A \right\}$.

If assumed as well that the initial unloaded strain state of the laminate corresponded to zero strains, namely, no residual stresses were present. Since the laminate is room temperature cured, it seems reasonable in this particular application (if initial or residual stresses were present, the applied vectors would radiate from a point different to the origin). Therefore, $\left\{ \epsilon_{ini} \right\} = 0$, and the corresponding strain response line **B** up to the actual strain state $\left\{ \epsilon_A \right\}$ (depicted with point **A**) may be plotted.

Proportional loading is assumed, so this response line **B** may be extended until its intersection with the failure criteria envelope in point **C**. The intersection would correspond to the failure strain state of the laminate (First Ply Failure is assumed), $\left\{ \epsilon_C \right\}$. The corresponding state of combined stresses, $\left\{ \sigma_C \right\}$, for the failure strain state, $\left\{ \epsilon_C \right\}$, may be obtained.

The proportional loading assumption allows to obtain an additional intersection point with the failure envelope, **T**. The corresponding stress vector $\left\{ \sigma_T \right\}$ for the failure strain $\left\{ \epsilon_T \right\}$ corresponds to the failure stress state of opposite sign to **C**. In the case of uniaxial longitudinal loading, i.e. point **C** would represent the failure for a compressive loading, while **T** the failure for a tensile loading.

The previously explained graphical procedure is transferred into an analytical formulation. A simple way for obtaining the failure stress state of the laminate may be achieved by means of a series of simple assumptions. A proper definition of the failure behaviour of the materials, and a known strain-stress state are required.

The general laminate theory for unsymmetric laminates is applied (see Sect. 2.1). The material properties allow to obtain the three stiffness matrices required for the complete definition of the laminate, $\left[A\right]$, $\left[B\right]$ and $\left[D\right]$.

The Tsai-Wu failure criteria is applied independently for the wood and the fibre. As explained in Sect. 2.2, the interaction factor $F^*_{xy} = 0.04$ is used for the wood, while the usually recommended [4], $F^*_{xy} = -0.5$, is applied for the composite reinforcement.

The elastic properties of the wood and the composite reinforcement are those derived in Sect. 3.1 (Table 2), obtained from the clear specimen testing and the explained formulations and ratios.

The internal stress vector is supposed to correspond to the applied loads. Only simple axial compressive forces are applied.The experimentally measured horizontal deformation is supposed to correspond only to that due to Poison coupling. No additional transversal stress or strain are assumed or, at least, they are considered as negligible.

To obtain the transversal strain, the Poison coefficient of the wood and FRP laminate is required. As explained in Sect. 2.1, it corresponds to the extension-

extension coupling represented by the A_{12} term on the laminate matrix. Therefore, it is necessary to know the stiffness matrix of the complete material, the wood plus the fibre reinforcement.

The thin layer assumption is employed. Kirchoff's hypothesis is applied, and second order displacements are dismissed. The previously explained normalized stiffness matrix [4], described in Sect. 2.1.1, is applied. The corresponding stress-strains equation is

$$\left\{ \begin{bmatrix} \sigma_i^0 \end{bmatrix} \right\} = \begin{bmatrix} \begin{bmatrix} A_{ij}^* \end{bmatrix} & \begin{bmatrix} B_{ij}^* \end{bmatrix} \\ 3 \begin{bmatrix} B_{ij}^* \end{bmatrix} & \begin{bmatrix} D_{ij}^* \end{bmatrix} \end{bmatrix} \left\{ \begin{bmatrix} \epsilon_j^0 \end{bmatrix} \right\} \tag{27a}$$

$$\begin{bmatrix} \sigma \end{bmatrix} = \begin{bmatrix} S^* \end{bmatrix} \begin{bmatrix} \epsilon \end{bmatrix} \tag{27b}$$

Taking advantage of the special properties of the normalized stiffness matrix (4), a particular internal stress state may be applied to the composite material. As explained, the internal stress state is simplified to correspond to the external loads. In the analysed case, since only axial compressive loading

is applied,

$$\left[\sigma_A\right] = \left\{\begin{array}{c} -1 \\ 0 \\ 0 \\ 0 \\ 0 \\ 0 \end{array}\right\} \tag{28}$$

may be assumed as the corresponding stress vector. The normalized formulation (4) in [4] is applied. Hence, the stress vector (28) represents an axial compressive stress state with a value of 1N/mm^2.

The equation system (27b) formed by the laminate stiffness matrix and the corresponding forces can then be solved to obtain the strains. Although only longitudinal stress ($\sigma_x = -1\text{N/mm}^2$ in $\left[\sigma_A\right]$) is assumed, strains in both longitudinal and transversal directions are produced due to the coupling terms present in the laminate matrix.

$$\left[\epsilon_A\right] = \left[S^*\right]^{-1} \left[\sigma_A\right] \tag{29}$$

The obtained strain vector, $\left[\epsilon_A\right]$ (point **A** in Fig. 8), corresponds to the previously assumed stress state (28), in which (in the depicted case) 1N/mm^2 in compression is applied. Two different analytical procedures are derived, and explained in the following sections.

4.3.1 Intersection alternative

As explained, linear response and proportional loading are assumed. Actual initial or residual stresses are dismissed. Consequently, the derived equation is based in the obtained strain point $\left[A \right]$ and the unloaded strain point, (0, 0). The equation of the response line in the strain space (**B** in Fig. 8) may be defined as:

$$\epsilon_y = \frac{\epsilon_{y.A}}{\epsilon_{x.A}} \epsilon_x \tag{30}$$

Having both the failure envelope for the laminate (10') and the behaviour of the material defined in the strain space by the response line (30), the intersection point between them may be obtained. This intersection depicts the failure strain, ϵ_f (**C** or **T** in the graphical application, Fig. 8). Two intersection points are obtained, for the assumed axial loading (axial compression, (28)) and the load of opposite sign (axial tension).

Proportional loading is assumed, therefore strain and stress are linearly related. The stress $\left\{ \sigma_f \right\}$ corresponding to this strain $\left\{ \epsilon_f \right\}$ may be easily computed from the ratio between known vectors $\left\{ \sigma_A \right\}$ and $\left\{ \epsilon_A \right\}$.

$$\left\{ \sigma_f \right\} = \frac{\sigma_{x.A}}{\epsilon_{x.A}} \left\{ \epsilon_f \right\}. \tag{31}$$

As the tube is submitted to simple axial loading, uniform stress distribution is considered. The failure compressive load may be obtained multiplying the failure stress σ_f by the area of the tube

$$F_f = A\sigma_f. \tag{32}$$

4.3.2 Strain Ratio alternative

The previously explained procedures are based on the intersection between what could be called the response line of the wood-fibre laminate(line BA) and the failure envelope (Fig. 8). A different analytical procedure may be obtained, based on the Strength Ratio definition (see Sect. 2.2.3).

The Strength Ratio represents the safety factor of the material, that is to say, how many times could be the applied load multiplied before failure. Consequently, if a unity stress were applied, the value of the corresponding Strength Ratio would be that of the failure stress. Since Laminate Theory assumes linear behaviour and relation among stress and strain, a similar Strain Ratio may be assumed, in which the actual applied strain is defined in relation to the failure strain as

$$R\epsilon_i|^{applied} = \epsilon_i|^{max}, \tag{33}$$

where $\epsilon_i|^{applied}$ would correspond to the strain vector referred as $\left\{\epsilon_A\right\}$ herein. Therefore, as it corresponds to a unity stress state, it would result that $R\left\{\epsilon_A\right\} \equiv \left\{\epsilon_f\right\}$.

The obtained strain state for a uniaxial compression stress, $\left\{\epsilon_A\right\}$, may be substituted in the strain failure criteria, and solve for R the resulting second order equation (similarly as described in (18)). Two different possible solutions arise. Tsai [11] stated in his Strength Ratio proposal (see Sect. 2.2.3) that only the positive root was possible. However, and as depicted in Fig. 8, the second negative root has, in this particular case, also a physical meaning. While the positive root corresponds to the uniaxial failure stress of the same

sign (compression or tension, the same as defined in the stress vector $\left\{ \sigma_A \right\}$, which corresponds to intersection point **C** in Fig. 8), the negative root, due the special uniaxial stress condition analysed here, stands for the uniaxial failure stress of the opposite sign. It would correspond to point **T** in the same Fig. 8. Consequently, this procedure allows to obtain the failure stress for both axial loading cases, uniaxial tension and compression.

As in the previous analytical procedure (see Sect. 4.3.1), since only axial stress is applied, the axial failure load corresponds to the area by the resulting failure stress, as shown in (32).

5 Application to the experimental results

The analytical model presented in the previous Sect. 4 is applied to the available experimental results described in Sect. 3.2. Applied fibre and wood properties are those shown in Table 2.

It is assumed that the reinforcement reduces the influence of the imperfections of the wood. Thus, in the case of the reinforced tubes, the strength values derived from the small clear specimens tests and the derived relations are employed in the analytical model.

However, conversely to man-made composite materials, wood, as a natural material, has a strong variability in its properties. It is well known how its strength is highly dependent on the occurrence of natural defects such as knots, compression wood and grain deviation. The reader interested in the subject is referred to [14,23] for further information. Consequently, and since

it is not the subject of this paper, a reduction factor γ_{unr} to take into account these imperfections is employed in the case of the unreinforced tube. A value of $\gamma_{unr} = 1.5$, which is seen as a good practical value for this issue, is chosen.

The corresponding model algorithm is programmed in *MatLab*. Both described analytical procedures, intersection (Sect. 4.3.1) and Strength Ratio (Sect. 4.3.2) are run.

Table 3 shows the resulting stiffness matrix for the CR85 and CR45 wood-fibre laminates. The material stiffness matrix corresponds to that of a balanced material, where the extension-shear is the only coupling not present. It may be seen how the in-plane–out-of-plane coupling elements are the more relevant terms in the $\left[B\right]$ matrix. The extension-twist coupling (B_{16} and B_{26}) are almost negligible. The bending-twist coupling may be considered of little importance in relation to the rest of the terms in matrix $\left[D\right]$. Both twist couplings have been shown not to be produced in axially loaded cylinders [8].

When the required unity stress vector (28) is applied, the corresponding strain state is obtained by solving equation (29). Resulting strains are presented in Table 4 for each of the analysed laminates. It may be seen how the longitudinal strain is the highest, since it is the direction of the applied load. While the longitudinal strain is similar for both laminates, about $6.1 \cdot 10^{-5}$, the transversal strain is about 35% higher for the CR45 laminate in comparison to the CR85. This fact, when the high anisotropy of wood is taken into consideration, is a negative effect for the wooden tubes.

The different required parameters for the Tsai-Wu criteria in strain space (10') for each of the materials are given in Table 5. Since only First Ply Failure is

Table 3

Normalized stiffness matrices of the CR85 and CR45 laminates

$$\left[A^*_{CR85}\right] = \begin{bmatrix} 16\,469.65 & 549.55 & 0.00 \\ 549.55 & 2\,627.04 & 0.00 \\ 0.00 & 0.00 & 953.97 \end{bmatrix}$$

$$\left[A^*_{CR45}\right] = \begin{bmatrix} 16\,738.40 & 773.75 & 0.00 \\ 773.75 & 1\,909.89 & 0.00 \\ 0.00 & 0.00 & 1\,178.17 \end{bmatrix}$$

$$\left[B^*_{CR85}\right] = \begin{bmatrix} -471.79 & 70.77 & -0.10 \\ 70.77 & 1\,206.25 & -2.07 \\ -0.10 & -2.07 & 108.27 \end{bmatrix}$$

$$\left[B^*_{CR45}\right] = \begin{bmatrix} -216.47 & 283.76 & -6.26 \\ 283.76 & 524.95 & -6.26 \\ -6.26 & -6.26 & 321.26 \end{bmatrix}$$

$$\left[D^*_{CR85}\right] = \begin{bmatrix} 15\,620.43 & 676.93 & -0.56 \\ 676.93 & 4\,798.30 & -11.83 \\ -0.56 & -11.83 & 1\,148.86 \end{bmatrix}$$

$$\left[D^*_{CR45}\right] = \begin{bmatrix} 16\,348.76 & 1\,284.52 & -35.66 \\ 1\,284.52 & 2\,854.80 & -35.66 \\ -35.66 & -35.66 & 1\,756.45 \end{bmatrix}$$

Table 4

Resulting strain vectors for the wood+FRP laminates

	CR85	CR45
ϵ_x	$6.14 \cdot 10^{-05}$	$6.1 \cdot 10^{-05}$
ϵ_y	$-1.7 \cdot 10^{-05}$	$-2.3 \cdot 10^{-05}$
$\gamma 7_{xy}$	$1.95 \cdot 10^{-08}$	$-1.3 \cdot 10^{-07}$
κ_1	$5.38 \cdot 10^{-06}$	$4.21 \cdot 10^{-06}$
κ_2	$9.67 \cdot 10^{-06}$	$-7.2 \cdot 10^{-06}$
κ_3	$1.79 \cdot 10^{-08}$	$4.12 \cdot 10^{-07}$

considered, the envelope of the wood is the only relevant in this study.

The obtained intersection point in the strain space between the failure envelope and the response line defined according to the strain vector (30) is given in Table 6. By means of the failure strain state and the ratio between the strain, the corresponding failure stress, may be obtained (31). Two different intersection points (corresponding to the axial compressive and tensional loading, respectively) among the response line and the failure envelope exist for each laminate (Table 6). The obtained failure stresses for each resulting failure strain state are given in Table 7.

The Strength Ratio procedure does not require to obtain the failure strain state. By solving the second order equation (18), as the initially applied stress ratio corresponds to a unity stress state, its result is the value of the failure stress. Two different values are obtained for each laminate. Coherently,

Table 5

Applied parameters of the Tsai-Wu criteria for the different materials, in SI units.

	Wood	±85 FRP	±45 FRP
G_{11}	133 045.18	13 057.58	6 423.81
G_{22}	134 812.48	10 036.35	6 423.81
G_{12}	55 205.40	−2 125.43	2 997.73
G_{66}	11 717.50	1 872.33	6 995.48
G_{16}	0.00	−1 036.53	−766.96
G_{26}	0.00	770.17	−766.96
G_1	333.74	39.90	25.28
G_2	605.70	10.66	25.28
G_6	0.00	−2.58	−14.84

Table 6

Failure strains according to the intersection procedure (10^{-3}).

	Compression		Tension	
	$\epsilon_{x.C}$	$\epsilon_{y.C}$	$\epsilon_{x.T}$	$\epsilon_{y.T}$
CR85	−3.78	1.07	2.35	−0.666
CR45	−3.50	1.34	2.58	−0.989

Table 7

Resulting analytical failure stresses, in N/mm^2

	σ_c	σ_T
CR 85	61.628	−38.221
CR 45	57.432	−42.335

Table 8

Analytical model: comparison to the experimental results

Experimental	Failure load [kN]			An.fail.stress
Exp. series	Ratio	Experimental	Analytical	[N/mm^2]
A				
*CR*85	0.9638	1044.50	1006.74	61.63
*CR*45	0.9829	954.50	938.19	57.43
REF (unr.)	0.9033	685.00	618.73	40.33
B				
*CR*090	1.1025	761.33	839.94	62.85
REF (unr.)	0.9643	534.00	514.95	40.33
	0.9834	Mean ratio		
	0.0731	Standard deviation		

the resulting failure stresses correspond to those obtained by the intersection procedure and shown in Table 7.

The predicted failure stress by the total transversal area of the tubes (32), considering both wood and FRP, gives the predicted axial failure load. The available experimental results were only to axial compressive loading. Therefore, at this stage, only the failure compressive load can be validated. Results in comparison to the experimental results are shown in Table 8. Series A tests are those in [3], 19mm thick and 1mm fibre reinforcement thick. Series B main difference with the previous series was the wood thickness of 16mm.

The analytical results are within an error less than 10%, with a mean error less than 3%. The standard deviation of the predictions of about 7%. A good correlation is thus observed with the axially loaded experiments of about 2.5m height.

6 Conclusions

A procedure of manufacturing wooden profiles has been developed and patented. Panels of densified wood are transformed to open or closed prismatic cross sections.The resulting profile encompasses efficient use of the material and optimal structural performance. An external layer of fibres is located at the outer side of the tubes, as reinforcement and protection from weathering.

The experimental test results of these reinforced columns to axial centred compression demonstrate that both load-carrying capacity and ductility are enhanced by means of the composite reinforcement. In average, the reinforced tubes reach a maximum load of about 1 000kN.The highest failure loads were

achieved for the columns with ±85° glass-fibre orientation (CR85), while the tubes reinforced with a ±45° cross-ply (CR45) feature more ductility. In comparison to the unreinforced reference, the load-carrying capacity of the reinforced columns increased by factors of 1.46 and 1.22 for the CR85 and CR45 tubes, respectively. In regard to the axial stiffness, the presence of reinforcement is negligible.

Herein, two different analytical procedures to obtain the axial failure strength of the material of the tubes have been presented: based on the intersection between the response line of the wood-fibre laminate and the failure envelope, or on the Strength Ratio definition.

The proposed algorithms apply the Classical Laminate Theory and the Tsai-Wu criteria. For the failure criteria, an adequate value for the interaction factor in the case of wood has been proposed. This value, $F^*_{xy} = 0.04$, is close to a zero value, and differs to a great extent to the proposal by Tsai [4].

The presented analytical models were applied to the available experimental results. The models are able to predict both compression and tension axial failure stresses, but only compressive failures have been experimentally done. Hence, only the failure compressive load was validated. Two different experimental campaigns were used for validation. The mean error was less than 3%, with a standard deviation of the predictions of about 3%. A good correlation is observed with the experiments and the anlytical procedures proposed herein.

The herein proposed analytical procedures have been calibrated and verified through the experimental data to assess their reliability. Predicted and experimental failure loads agreed reasonably well. Therefore, the proposed procedures are an adequate tool for the design and optimisation of wooden rein-

forced tubes. However, more sophisticated analytical models have to be developed and further tests on tubes with varying $\frac{r}{t}$ and $\frac{l}{r}$ ratios are required in the future.

7 Acknowledgements

The Alexander von Humboldt Foundation is gratefully acknowledged for providing sponsorship to the first author. Furthermore, the authors would like to thank the German Federal Ministry of Education and Research (BMBF - Project: "High-Performance Timber Structures" Nr. 0330722A) for supporting this research.

References

[1] P. Haller, Concepts for textile reinforcements for timber structures, Materials and Structures 40 (2007) 107–118.

[2] A. Heiduschke, J. M. Cabrero, C. Manthey, P. Haller, E. Günther, Mechanical behaviour and life cycle assessment of fibre-reinforced timber profiles, in: L. Braganca, H. Koukkari, H. Blok, R.and Cervasio, M. Velkovic, R. U. V. Plewako, Z.and Landolfo, L. Silva, P. Haller (Eds.), COST C25 Sustainability of Constructions - Integrated Approach to Lifetime Engineering, COST C-25, European Commission, Dresden, 2008, pp. 3.38–3.46.

[3] A. Heiduschke, P. Haller, Zum tragverhalten gewickelter formholzrohre unter axialem druck, Bauingenieur 84 (6) (2009) 262–269.

[4] S. W. Tsai, Theory of Composites Design, Think Composites, Dayton, 1992.

[5] W. Michaeli, D. Huybrechts, M. Wegener, Dimensionieren mit Faserverbundkunststoffen: Einführung und praktische Hilfen, Hanser, München, 1995.

[6] L. P. Kollár, G. S. Springer, Mechanics of composite structures, Cambridge Univ. Press, 2003.

[7] H. W. Bergmann, Konstruktionsgrundlagen für Faserverbundbauteile, Springer, 1992.

[8] G. Eckold, Failure Criteria in Fibre reinforced Polymer Composites: The World-Wide Failure Exercise, Elsevier, 2004, Ch. Failure criteria for use in the design environment, pp. 121–139.

[9] T. V. der Put, The tensorpolynomial failure criterion for wood, Tech. rep., Delft Wood Science Foundation (2005).

[10] J. Eberhardsteiner, Mechanisches Verhalten von Fichtenholz: experimentelle Bestimmung der biaxialen Festigkeitseigenschaften, Springer, 2002.

[11] K.-S. Liu, S. Tsai, Failure Criteria in Fibre reinforced Polymer Composites: The World-Wide Failure Exercise, Elsevier, 2004, Ch. A progressive quadratic failuer criterion for a laminate, pp. 334–352.

[12] Deutsches Institut für Normung, DIN 52186: Prüfung von Holz. Biegeversuch, Deutsches Institut für Normung, 1978.

[13] Deutsches Institut für Normung, DIN 52185: Prüfung von Holz. Bestimmung der Druckfestigkeit parallel zur Faser, Deutsches Institut für Normung, 1976.

[14] J. Bodig, B. Jayne, Mechanics of Wood and Wood Composites, Van Nostrand Reinhold, New York, 1982.

[15] CEN, prEN 1995: Design of Timber Structures, CEN, 2004.

[16] Deutsches Institut für Normung, DIN 1052:2004. Entwurf, Berechnung und Bemessung von Holzbauwerken, Deutsches Institut für Normung, Berlin, 2004.

[17] U. Kuhlmann, P. Aldi, Simulation of grooved connections in timber-concrete composite beams considering the distribution of the material properties, in: 10th World Conference on Timber Engineering (WCTE 2008). Conference Preceedings, WCTE, Miyazaki, Japan, 2008.

[18] H. Blaß, M. Schmid, Querzugfestigkeit von vollholz und brettschichtholz, Holz als Roh- und Werkstoff 58 (2001) 456–466.

[19] Fiberline Composites A/S, Fiberline Design Manual, 2nd Edition, 2003.

[20] G. Simitses, Buckling of moderately thick laminated cylindrical shells: a review., Composites Part B 27B (1996) 581–587.

[21] L. Čábi, Stütze aus formholz, Bericht zur Doktorarbeit im Ausland, Fakultät Bauingenieurwesen. Stahl- und Holzbau Institut. Technische Universität Dresden (2006).

[22] H. Altenbach, J. Altenbach, W. Kissing, Mechanics of Composite Structural Elements, Springer, 2004.

[23] J. M. Dinwoodie, Timber: its nature and behaviour, 2nd Edition, Taylor & Francis, 2000.